

## The $\beta$ amyloid peptide can act as a modular aggregation domain

Christopher D. Link<sup>a,\*</sup>, Virginia Fonte<sup>a</sup>, Christine M. Roberts<sup>a</sup>, Brian Hiester<sup>a</sup>,  
Michael A. Silverman<sup>b</sup>, Gretchen H. Stein<sup>c</sup>

<sup>a</sup> Institute for Behavioral Genetics, University of Colorado, Boulder, CO 80309, USA

<sup>b</sup> Biological Sciences, Simon Fraser University, Burnaby, Canada BC V5A 1S6

<sup>c</sup> Molecular, Cellular, and Developmental Biology, University of Colorado, Boulder, CO 80309, USA

### ARTICLE INFO

#### Article history:

Received 1 February 2008

Revised 15 July 2008

Accepted 5 August 2008

Available online 22 August 2008

#### Keywords:

Alzheimer's disease

*C. elegans*

Transgenic

Neurodegeneration

$\gamma$ -secretase

$\alpha$ -secretase

AICD

### ABSTRACT

Although there is compelling evidence that the  $\beta$  amyloid peptide ( $A\beta$ ) can be centrally involved in Alzheimer's disease, the natural role (if any) of this peptide remains unclear. Here we use green fluorescent protein (GFP) fusions to demonstrate that the  $A\beta$  sequence, like prion domains, can act as a modular aggregation domain when terminally appended to a normally soluble protein. We find that a single amino acid substitution (Leu<sup>17</sup> to Pro) in the  $\beta$  peptide sequence can abolish this *cis* capacity to induce aggregation. Introduction of this substitution into full-length APP (i.e., a Leu<sup>613</sup>Pro substitution in APP695) alters the processing of APP leading to the accumulation of the C99 C-terminal fragment (CTF). We suggest that in at least some aggregation disease-related proteins the presence of an aggregation domain is not "accidental", but reflects a selected role of these domains in modulating the trafficking or metabolism of the parental protein.

© 2008 Elsevier Inc. All rights reserved.

### Introduction

The  $\beta$  amyloid peptide ( $A\beta$ ), which is likely to be centrally involved in Alzheimer's disease (AD) pathology (Hardy and Selkoe, 2002), has an inherent capacity to multimerize and aggregate *in vitro* and *in vivo* (Finder and Glockshuber, 2007). It is unknown if the capacity of the  $\beta$  amyloid peptide to multimerize rapidly and aggregate serves a selected function, or if this aggregation ability is an unselected consequence of some other selected capacity. Other larger proteins associated with neurodegenerative diseases, such as prion protein (PrP) and polyglutamine repeat-containing proteins (e.g., huntingtin) show similar aggregation capacities (Koo et al., 1999). The aggregation of polyglutamine repeat proteins depends specifically on the repeat sequence; addition of long polyglutamine repeats to normally soluble proteins, such as Green Fluorescent Protein (GFP), causes aggressive aggregation of the fusion protein (Moulder et al., 1999; Satyal et al., 2000). Similarly, molecular dissection of yeast prion proteins has demonstrated that a glutamine/asparagine-rich domain is responsible for their aggregation, and this domain can convey aggregation when fused to heterologous soluble proteins (DePace et al., 1998; Li and Lindquist, 2000; Osherovich and Weissman, 2001; Osherovich et al.,

2004). Si et al. identified a neuronal isoform of the *Aplysia* CPEB protein that contains a glutamine/asparagine-rich domain that can likewise convey prion-like properties when fused to heterologous proteins and expressed in yeast (Si et al., 2003). These authors suggested that the conversion of CPEB to a prion-like state might be important for the function of this protein, as it could allow the establishment of a localized, stable epigenetic switch important for maintaining long-term synaptic changes.

The  $A\beta$  peptide is derived by proteolytic cleavage from the Amyloid Precursor Protein (APP), a broadly expressed protein with multiple functions, including a proposed role in synaptic function (Kamenetz et al., 2003). By analogy with the glutamine/asparagine-rich domain of CPEB, the  $A\beta$  peptide sequence could function as an aggregation domain and play a role in the function of its "host" protein, APP. We therefore sought to determine 1) if the  $A\beta$  sequence could serve as a transferable aggregation domain module, and 2) if interference with the proposed aggregation capacity of the  $A\beta$  sequence could modulate APP function. We find that the  $A\beta$  sequence can act as an aggregation module, and that APP processing is altered by introduction of a mutation in the  $A\beta$  domain that abrogates its aggregation potential.

### Methods

#### Construction of transgenes and transgenic strains

The human  $A\beta$  3–42 sequence was cloned in frame downstream of GFP in *C. elegans* expression vectors that use either the *myo-3*

\* Corresponding author. Fax: +1 303 492 8063.

E-mail address: [linkc@colorado.edu](mailto:linkc@colorado.edu) (C.D. Link).

Available online on ScienceDirect ([www.sciencedirect.com](http://www.sciencedirect.com)).

promoter to drive muscle-specific expression or the *snb-1* promoter to drive pan-neuronal expression. An equivalent mammalian expression vector was constructed by inserting the A $\beta$  3–42 sequence downstream of GFP in the CMV-driven expression vector EGFP-C2 (Clontech). The Leu<sup>17</sup>Pro mutation was introduced into the *C. elegans* and mammalian expression constructs (including APP695 and C99-GVP) by *in vitro* mutagenesis (Gene Tailor kit, Invitrogen). Transgenic *C. elegans* lines were established by microinjection as previously described (Link, 1995; Fay et al., 1998), using either pRF4 (dominant *rol-6* morphological marker) or pCL26 (intestinal GFP expression) as selected markers.

#### Biochemical measurements of GFP::A $\beta$ aggregation

Sequential extraction of nematode tissue and filter trap assays were performed as previously described (Link et al., 2006). For the sequential extraction experiments, nematode homogenates were prepared in Tris/Triton X-100 immunoprecipitation buffer (Fonte et al., 2002), then initially extracted for 1 h (4 °C) in Tris/glycerol buffer containing protease inhibitors. Insoluble material was pelleted by centrifugation (25,000  $g \times 15$  min) and re-extracted in 1% SDS (1 h, 4 °C). The remaining insoluble material was pelleted (25,000  $g \times 15$  min centrifugation). Extracts were concentrated, desalted, and fractionated on 4–12% Bis-Tris gels. Immunoblots were performed with anti-GFP antibody (Qbiogene).

The filter trap assays were performed using Tris/Triton X-100 nematode homogenates cleared of large insoluble material (i.e., cuticle fragments) by low-speed spin (5 min at 325 relative centrifugal force). Replicate homogenate aliquots (5  $\times$  30  $\mu$ l) were run through a 0.2  $\mu$ m cellulose acetate membrane pre-soaked in

immunoprecipitation buffer. After drying, identical circular punches of the membrane were transferred to flat-bottom wells of a 96-well microtiter plate and total trapped GFP fluorescence was quantified using a microplate reader. Relative trapped GFP fluorescence (Fig. 1H) was calculated by averaging total GFP fluorescence (arbitrary units from Tecan GENios microplate reader) from replicate wells and subtracting the background signal from homogenate-only punches.

#### Hippocampal cell culture and transfection

Primary cultures of dissociated neurons from E18 embryonic rat hippocampi were prepared essentially as described (Banker and Goslin, 1998). Cells were maintained in Neurobasal medium (Life-Tech/GIBCO-BRL) supplemented with B-27 and Glutamax. After 7 days *in vitro*, cells were transfected with 2.0  $\mu$ g of plasmid DNA using Lipofectamine 2000 (Invitrogen, No. 11668-019), per the manufacturer's instruction. Cells were maintained in a 37 °C/5% CO<sub>2</sub> incubator for 12 or 24 h to allow protein expression. Immunofluorescence and microscopy of hippocampal cells. Cells were fixed in a solution of 4% paraformaldehyde/4% sucrose in PBS, then blocked in 0.5% fish skin gelatin in PBS for 1 h at 37 °C. After blocking, coverslips were incubated with a polyclonal MAP2 (Chemicon #AB5622, 1:500) antibody overnight at 4 °C, which was followed by incubation in Cy3-conjugated goat anti-rabbit (Jackson Labs, 1:500) for 1 h at 37 °C. Coverslips were mounted on glass slides in Elvanol containing 0.5  $\mu$ g/ml DAPI. Images of GFP expressing cells were acquired using a SPOT RT-SE (Diagnostics Instruments) cooled CCD camera controlled by Metamorph Software (Universal Imaging) with a 60 $\times$ , 1.4 N.A. Plan Apo objective (Nikon).

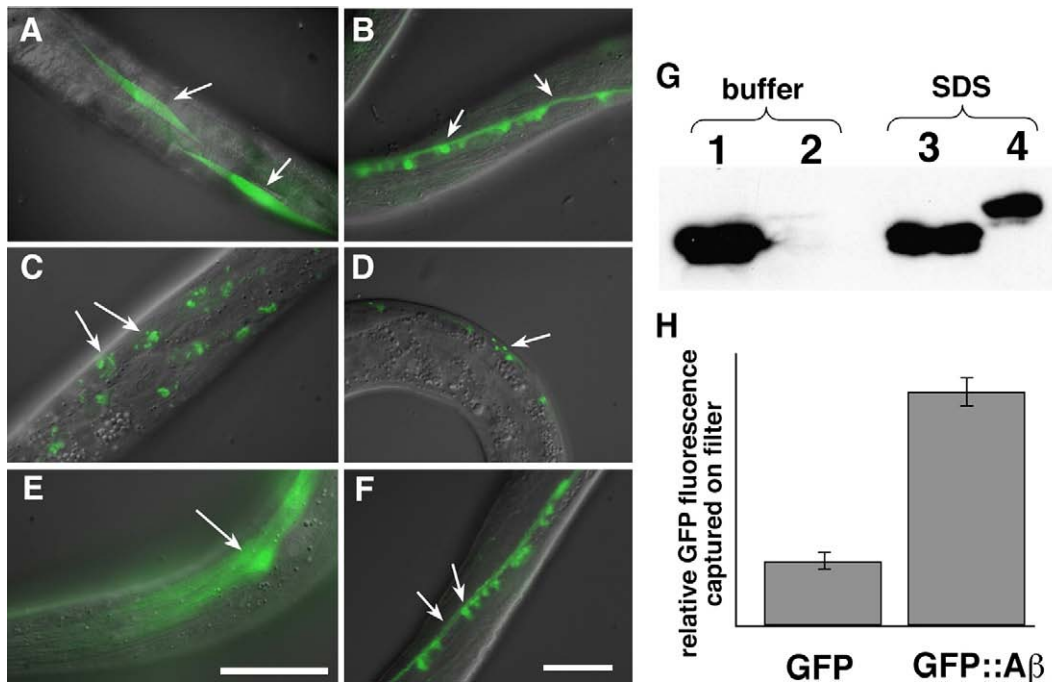


**Fig. 1.** Aggregation of GFP::A $\beta$  fusion protein expressed in *C. elegans*. Panels A–F, fused DIC/epifluorescence images of live transgenic worms. (A) *C. elegans* strain (CL1179, *myo-3*/GFP transgene) with body wall muscle expression of GFP. Note the even cytoplasmic GFP accumulation in spindle-shaped muscle cells (arrows). (B) *C. elegans* strain (CL1234, *snb-1*/GFP) with GFP expression in ventral cord neurons. Note GFP accumulation in neuronal cell bodies and axons (arrows). (C) *C. elegans* strain (CL1332, *myo-3*/GFP::A $\beta$ ) with body wall muscle expression of the GFP::A $\beta$  fusion protein. Note perinuclear GFP aggregates (arrows). (D) *C. elegans* strain (CL1358, *snb-1*/GFP::A $\beta$ ) with GFP::A $\beta$  expression in ventral cord neurons. Note GFP fluorescence is restricted to cell body aggregates (arrow). (E) *C. elegans* strain (CL1364, *myo-3*/GFP::A $\beta$  Leu<sup>17</sup>Pro) with body wall muscle expression of substituted GFP::A $\beta$  fusion protein. Note restoration of diffuse cytoplasmic GFP fluorescence (arrow). (F) *C. elegans* strain (CL1363, *snb-1*/GFP::A $\beta$  Leu<sup>17</sup>Pro) with expression of substituted GFP::A $\beta$  fusion protein in ventral cord neurons. Note restoration of GFP fluorescence throughout neuronal cell bodies and axons (arrows). Size bars = 50  $\mu$ m. (G) Reduced solubility of GFP::A $\beta$ . Disrupted transgenic worms expressing body wall muscle GFP (lanes 1 and 3) or GFP::A $\beta$  (lanes 2 and 4) were sequentially extracted with Tris pH8.6/10% glycerol buffer and then 1% SDS. Note a significant fraction of GFP is recovered in the Tris/glycerol wash, but measurable recovery of GFP::A $\beta$  requires detergent extraction. (H) Preferential recovery of GFP::A $\beta$  by filter trap assay. Cleared homogenates of transgenic worms expressing body wall muscle GFP or GFP::A $\beta$  were passed through a 0.2  $\mu$ m cellulose acetate filter, and retained GFP was assayed by fluorimetry. Bars represent the the average GFP signal (arbitrary units) of 5 replicate assays,  $\pm$ S.E.M. Note increased retention of GFP::A $\beta$ .

### CHO cell transfections and luciferase assay

CHO cells were seeded at 50,000 cells/cm<sup>2</sup> in 24-well tissue culture plates (2 cm<sup>2</sup>/well) in Ham's F12 supplemented with 10% FBS. One day later, when the cells were approximately 90% confluent, each well was transfected with Lipofectamine 2000 (Invitrogen) together with 100 ng CMV- $\beta$ gal, 100 ng MH100 (UAS-luciferase) and 100 ng of C99/GVP, pCL120 (C99/GVP-L17P) or empty vector pcDNA3.1. All of the plasmids except CL120 were a gift from A. Bergman (Karolinska Institutet), and the luciferase assays were done 18–24 h post-transfection essentially as described (Bergman et al., 2003). Briefly, cell lysates were prepared, clarified by centrifugation, and kept on ice while aliquots of each lysate were added to tubes containing ATP and D-luciferin, mixed and read luminometrically exactly 20 s after mixing, alternating between control and experimental samples. A second aliquot of each lysate was used to measure  $\beta$ gal activity as an indicator of transfection efficiency. The luciferase results were normalized to the  $\beta$ gal activity, and statistical significance was determined by Student's *t*-test: Two sample assuming equal variances.

### Biotinylation of CHO cell surface proteins

CHO cells were transfected with CMV- $\beta$ gal and either full-length wildtype APP695 or CL146 (APP-Leu613Pro) DNA. At 24 h after transfection, the cells were biotinylated for 30 min at 4 °C using the Pierce Cell Surface Protein Isolation Kit #89881. The cells were harvested by scraping, lysed, and used for immunoblots and determination of transfection efficiency as described above. Transfection efficiencies were approximately equal (APP-Leu613Pro was 92–99% of APP695).

### Immunoblots

$\beta$  galactosidase assay of transfection efficiency was used to normalize samples. Protein was quantitated by a Bradford assay (Pierce), and 20  $\mu$ g of sample were loaded per lane. SDS-PAGE sample buffer was used (62.5 mM Tris pH 6.8, 1%SDS, 10% glycerol, 2.5% 2-Mercaptoethanol, and 0.02% bromophenol blue), and samples were run at 180 V on NuPAGE 4–12% Bis–Tris Gel (Invitrogen, NP0321) using MES SDS Running Buffer (Invitrogen NP0002). Gels were transferred to 0.45  $\mu$  supported nitrocellulose (GE Osmonics WP4HY00010) using 20% methanol, 39 mM glycine, 48 mM Tris base. Transfer conditions were 21 V, 108 min. Prestained Rainbow size markers (Amersham Biosciences RPN755, RPN800) were used to size bands.

Blots were visualized by Ponceau stain, and then boiled for 3 min in PBS. Blots were blocked in TBS-Tween +5% milk (100 mM Tris7.5, 150 mM NaCl, 0.1% Tween-20). APP C-terminal antibody CT20 (rabbit polyclonal, gift of C. Eckman) was diluted 1:5000 in blocking solution. Secondary antibody was HRP-conjugated goat anti-rabbit IgG (Sigma) diluted 1:2000. Mouse monoclonal anti-A $\beta$  (Chemicon, 6E10) was diluted 1:1000 in blocking solution. N-terminal APP mouse monoclonal antibody (Chemicon, 22C11) was diluted 1:1000 in PBS-0.1% Tween+1% BSA. Actin monoclonal antibody JLA20 (Developmental Studies Hybridoma Bank, University of Iowa) was diluted 1:100 in blocking solution. Secondary HRP-conjugated goat anti-rabbit or anti-mouse IgG (Sigma) was diluted 1:2000. Immunoblots were visualized using ECL (Amersham).

### ELISA for A $\beta$ 40 peptides

CHO cells were transfected with CMV- $\beta$ gal and either full-length wildtype APP695 or CL146 (APP-Leu613Pro) DNA. The medium was changed at 6 h, collected at 24 h, and analyzed with a Biosource ELISA kit for human A $\beta$ 40 (Invitrogen). The results were normalized to the transfection efficiency of the cells, as determined by  $\beta$ gal activity.

## Results

### GFP::A $\beta$ fusion proteins aggregate in invertebrate and mammalian cells

GFP expressed in *C. elegans* tissues remains cytoplasmic and soluble, even when its expression is driven by high-level promoters (e.g., see Figs. 1A and B). Conversely, intracellular expression of A $\beta$  1–42 in *C. elegans* results in the formation of immunoreactive deposits and amyloid fibrils (Link et al., 2001). We fused A $\beta$  sequences 3–42 in frame to the C-terminus of GFP, using a convenient EcoRI site present in the A $\beta$  sequence. This GFP::A $\beta$  fusion protein was expressed either in body wall muscle or pan-neuronally, using the promoters from the *C. elegans myo-3* and *snb-1* genes, respectively. In both muscle and neurons, addition of the A $\beta$  sequence to GFP results in a dramatic redistribution of the GFP into perinuclear aggregates, readily visible in live animals (Figs. 1C and D). To determine if the visible aggregation correlated with decreased solubility of the GFP::A $\beta$  fusion, protein lysates from transgenic animals with muscle expression of GFP or GFP::A $\beta$  were sequentially extracted using salt and SDS-containing buffers. As shown in Fig. 1G, efficient recovery of GFP::A $\beta$ , but not GFP, requires strong detergent extraction. The insolubility of GFP::A $\beta$  was also demonstrated by filtration of worm lysates through 0.2  $\mu$ m cellulose acetate filters (Link et al., 2006), where GFP::A $\beta$  is significantly better retained than GFP (Fig. 1H). We also attempted to stain GFP::A $\beta$  deposits with the amyloid-specific dye X-34, which can be used to visualize  $\beta$ -amyloid deposits in living *C. elegans* worms (Link et al., 2001). However, we did not see specific staining of GFP::A $\beta$  deposits, suggesting that addition of the A $\beta$  peptide to GFP cannot drive this normally globular protein into amyloid fibrils (data not shown).

To investigate whether the aggregation-induction capacity of A $\beta$  also occurs in mammalian neurons, we constructed an analogous expression vector using CMV promoter-driven EGFP, and transiently transformed primary fetal rat hippocampal neurons. While transformation with an unmodified EGFP expression construct resulted in neurons with EGFP fluorescence throughout the cell body, dendrites, and axons, neurons transformed with EGFP::A $\beta$  had their EGFP fluorescence restricted to the perinuclear region. This restricted distribution was observed at all timepoints and in apparently healthy neurons with intact axons (Fig. 2).

A Leu<sup>17</sup>Pro substitution in the A $\beta$  sequence interferes with A $\beta$  fusion-induced aggregation. We have previously identified substitutions in the A $\beta$  1–42 sequence that blocked amyloid formation in the *C. elegans* model system (Fay et al., 1998). One such substitution, Leu<sup>17</sup>-to-Pro, targets a central hydrophobic region thought to be critical for A $\beta$  aggregation. This same substitution was subsequently identified in an elegant unbiased study that employed random mutagenesis to reverse the misfolding of an A $\beta$ ::GFP fusion protein expressed in *E. coli* (Wurth et al., 2002). We introduced the Leu<sup>17</sup>Pro substitution into our *C. elegans* and mammalian GFP::A $\beta$  expression vectors by *in vitro* mutagenesis, and found that this substitution countered the A $\beta$  fusion-induced aggregation in all cases (Figs. 1E and F; 2C).

### Influence of the A $\beta$ sequence on APP processing and signaling

$\beta$ -secretase processing of APP results in a 99 residue C-terminal fragment (C99) containing the A $\beta$  sequence at its N-terminus. We hypothesized that this terminal A $\beta$  sequence, via its multimerization capacity, might be able to influence subsequent processing of the APP C99 fragment, specifically its cleavage by  $\gamma$ -secretase. To test this hypothesis, we introduced a Leu<sup>613</sup>Pro substitution (equivalent to the Leu<sup>17</sup>Pro A $\beta$  substitution) into an APP695 expression construct and transfected CHO cells with wild type or Leu<sup>613</sup>Pro APP. Transfected cells were subsequently surface-labeled with biotin hydrazide to allow measurement of both total and cell surface APP and APP processing products. As shown in Fig. 3, immunoblot analysis using an antibody specific for the C-terminus of APP revealed that the Leu<sup>613</sup>Pro

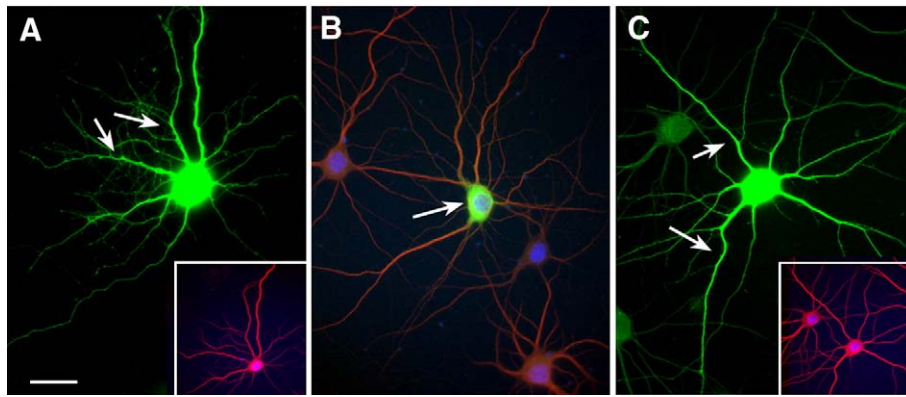


**Fig. 2.** Expression of GFP and GFP fusion proteins in primary rat neurons. Primary cultures of dissociated neurons from E18 embryonic rat hippocampi were transfected with CMV promoter-driven expression vectors expressing GFP (panel A), GFP::A $\beta$  (panel B), or GFP::A $\beta$  Leu<sup>17</sup>Pro (panel C). Transfected cultures were fixed and stained with anti-MAP2 (red) antibody and DAPI (blue). Note expressed GFP extends from the cell body to the axon and dendrites (arrows, panel A), while GFP::A $\beta$  remains localized to the neuronal cell body (arrow, panel B). In contrast, GFP::A $\beta$  Leu<sup>17</sup>Pro fluorescence is distributed throughout the neuron as observed for unmodified GFP (arrows, panel C). MAP2 staining, a marker for dendrites, is shown in corner insets (panels A and C) or as fused image (panel B). Size bar = 25  $\mu$ M.

substitution leads to a strong increase in both total and cell surface C99, without appreciable effects on the accumulation of full-length APP. Accumulation of the C99 fragment in cells transfected with APP695 Leu<sup>613</sup>Pro suggests that this substitution leads to reduced  $\gamma$ -secretase processing.

$\gamma$ -secretase cleavage of APP leads to the release of an intracellular cytoplasmic domain (AICD) that can subsequently translocate to the nucleus and influence gene expression (Kimberly et al., 2001; Leissring et al., 2002). In the experiment described above, we were unable to detect AICD (i.e., C59 or shorter peptides that result from  $\gamma/\epsilon$  cleavage) in any of the transfected cells, likely due to the very short *in vivo* half-life of this peptide (Cupers et al., 2001). We

therefore turned to a sensitive reporter system to determine if the increased accumulation of C99 in cells transfected with APP695 Leu<sup>613</sup>Pro is mirrored by a decreased production of AICD, as is predicted to result from reduced  $\gamma$ -secretase activity. Karlstrom and colleagues have developed a chimeric reporter construct (C99-GVP) to measure this processing/signaling event by inserting a Gal4VP16 transactivator sequence into the AICD portion of APP C-terminal fragment (Karlstrom et al., 2002; Bergman et al., 2003). Co-transformation of CHO cells with C99-GVP and a UAS-luciferase reporter allows the amount of APP processing to be measured quantitatively by assaying luciferase activity. As shown in Fig. 4A, introduction of the Leu<sup>17</sup>Pro-equivalent substitution into C99-GVP significantly decreased processing as measured by luciferase activity. This reduced release of AICD is associated with an increased accumulation of unprocessed C99-GVP Leu<sup>17</sup>Pro (Fig. 4B), consistent with reduced  $\gamma/\epsilon$ -secretase activity.

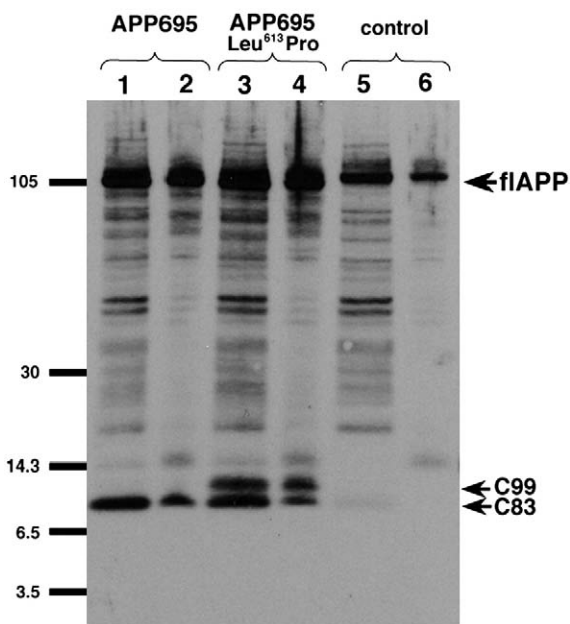


**Fig. 3.** Effect of Leu-to-Pro substitution on APP processing. CHO cells were transfected with APP695 or APP695 Leu<sup>613</sup>Pro. The cells were subjected to cell surface biotinylation 24 h after transfection, then harvested. Total cell extracts or biotinylated material were fractionated by SDS-PAGE and probed with CT-20 antisera, which recognizes the C-terminus of APP. Lanes 1, 3, and 5 contain whole cell extracts; lanes 2, 4, and 6 contain biotinylated cell surface material. Note specific accumulation in both total and cell surface fractions of APP C99 fragment in APP695 Leu<sup>613</sup>Pro transfected cells, despite levels of full-length APP (flAPP, ~105 kDa) similar to that expressed in APP695 transfected cells. (The C99 band, but not the C83 band, was recognized by mAb 6E10, confirming that this fragment retains the N-terminal portion of A $\beta$ .)

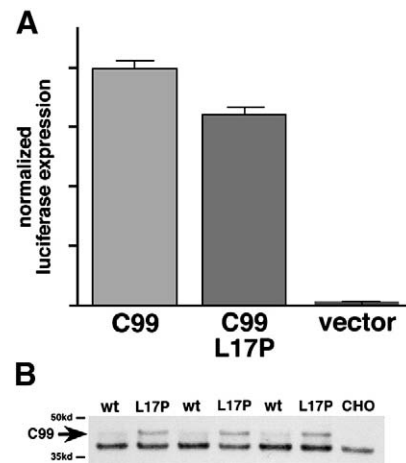


**Fig. 4.** Effect of Leu<sup>17</sup>-to-Pro substitution on release of APP intracellular domain. (A) CHO cells were co-transfected with either the C99-GVP or C99-GVP Leu<sup>17</sup>Pro reporter constructs (along with UAS/luciferase and a CMV/ $\beta$ -galactosidase plasmid for normalization of transfection efficiencies), harvested 24 h later, and luciferase activities of cell extracts were determined. (Results are from 6 independent transfection experiments.) Note ~20% decrease in luciferase activity associated with transfection with C99-GVP Leu<sup>17</sup>Pro (arbitrary luciferase activity units; error bars = S.E.M.;  $p < 0.05$ ). (B) Extracts of CHO cells transfected in triplicate as described above were fractionated by SDS-PAGE and probed with mAb 6E10, which recognizes residues 1–16 of A $\beta$ . Note the accumulation of unprocessed C99-GVP specifically in cells transfected with the mutant reporter construct. [The unprocessed C99-GVP runs at ~45 kd due to the addition of the Gal4-VP16 transactivator domains (19)].

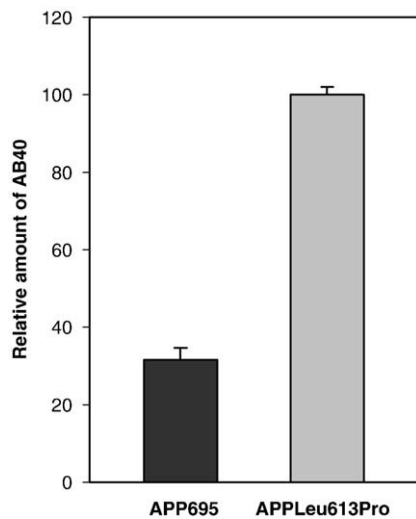


**Fig. 5.** Effect of Leu-to-Pro substitution on Aβ<sub>40</sub> production. CHO cells were transfected with APP695 or APP695 Leu<sup>613</sup>Pro, and the amount of Aβ<sub>40</sub> released into the medium between 6–24 h was analyzed by an ELISA for human Aβ<sub>40</sub>. Note that cells expressing APP695 Leu<sup>613</sup>Pro secreted approximately 3-fold more Aβ<sub>40</sub> than did cells expressing wildtype APP ( $p < 0.001$ ).

Although the results described above support an effect of the Leu<sup>17</sup>Pro substitution on  $\gamma/\epsilon$  cleavage of APP, they do not account for the preferential accumulation of the C99 APP fragment in comparison to accumulation of the APP C83 fragment (Fig. 3). One possible explanation for this observation is that the Leu<sup>17</sup>Pro substitution reduces  $\alpha$ -secretase cleavage of APP. Elevated  $\alpha$ -secretase levels have been shown to increase AICD production (Kume et al., 2004), and analysis of long Aβ-related peptides has demonstrated that  $\epsilon$ -cleavage depends on  $\alpha$ -secretase pre-cutting (Kametani, 2004). Thus, the Leu<sup>17</sup>Pro substitution may secondarily decrease  $\gamma/\epsilon$  cleavage by interfering with  $\alpha$ -secretase cleavage. To test this hypothesis, we measured secreted Aβ 1–40 from CHO cells transfected with APP695 or APP695 Leu<sup>613</sup>Pro using an ELISA assay that only detects full-length Aβ 1–40. Given that the Leu<sup>613</sup>Pro substitution has a significantly stronger effect on C99 accumulation than on AICD reduction (i.e.,  $\gamma/\epsilon$  cleavage), we would predict that reduced  $\alpha$ -secretase cleavage of this APP variant would lead to a net overall increase in Aβ secretion. As shown in Fig. 5, transfection with APP695 Leu<sup>613</sup>Pro does lead to an approximately three-fold accumulation of secreted Aβ 1–40.

## Discussion

Our studies show that fusion of the Aβ sequence (specifically residues 3–42) to a heterologous protein can induce the aggregation of the fusion protein, as has been previously demonstrated for polyglutamine repeats and glutamine/asparagine-rich domains from prion proteins. However, Aβ has neither sequence nor predicted structural similarities to these other aggregation domains, and is thus likely to function by a different molecular mechanism. Nevertheless, an overriding question for all these classes of aggregating proteins is whether the presence of the respective aggregation domains in their natural context is important for the function of the host proteins. In the case of yeast prion [PSI<sup>+</sup>], it appears that while the prion domain is not necessary for the biochemical function of this protein *per se* (Ter-Avanesyan et al., 1993), the metastable epigenetic state conferred by the prion domain can confer selective advantages in changing environments (True and Lindquist, 2000). Of perhaps more relevance to APP are the studies of the neuronal isoform of the *Aplysia* CPEB protein, which have led to the provocative suggestion that the prion-like domain of this protein may function as a self-perpetuating epigenetic switch to maintain activated CPEB in localized synaptic

regions (Si et al., 2003). We know of no evidence indicating that the Aβ sequence has true prion-like functions [although small Aβ aggregates can efficiently seed amyloid fibril formation (Jarret and Lansbury, 1993)]. However, the general model that localized aggregation/multimerization is a mechanism for modulating protein function may be applicable to APP.

The relationship between a protein's conformation *in vivo* and its subsequent metabolism is difficult to assay directly, in part because of the difficulty of monitoring the *in vivo* conformation of specific proteins without the addition of components (e.g., FRET probes) that might by themselves alter protein metabolism. We have therefore taken the approach of engineering specific amino acid substitutions that have demonstrable effects on *in vivo* protein conformation and determining the effects of these substitutions on protein metabolism. Using this approach, we have generated data suggesting that the propensity of the Aβ peptide sequence to drive multimerization may influence  $\alpha$ - and  $\gamma/\epsilon$ -secretase processing of APP. We have not, however, directly demonstrated that the APP695 Leu<sup>613</sup>Pro mutation interferes with APP multimerization (e.g., by cross-linking studies).

There is evidence that APP forms homodimers and homotetramers *in vivo*, and that this association is mediated at least in part by two conserved regions in the APP ectodomain (Scheuermann et al., 2001). Furthermore, forced dimerization of APP by introduction of a Lys<sup>624</sup>Cys substitution (resulting in intermolecular disulfide bond formation) was found to increase dramatically the production of Aβ in transfected SY5Y cells, indicating that the multimerization state of APP can profoundly affect its processing. Both the extracellular loop of APP (Kaden et al., 2008) and the GxxxG motif in its transmembrane portion (Munter et al., 2007) have also been implicated in the dimerization and  $\gamma$ -secretase processing of APP. Our results suggest that the extracellular portion of the Aβ sequence (including Leu<sup>17</sup>) may also play a role in the multimerization of APP, with subsequent effects on  $\alpha$ - and  $\gamma/\epsilon$ -secretase processing. In this regard, substitutions at Ser26 and Leu28 have also been shown to impair  $\gamma$ -secretase-dependent cleavages (Ren et al., 2007).

The reduction of  $\alpha$ -secretase cleavage of APP695 by the Leu<sup>613</sup>Pro substitution could be the result of this substitution simply altering a consensus protease cleavage site recognized by  $\alpha$ -secretase. However, the membrane-associated metalloproteases believed to act as  $\alpha$ -secretases (ADAM9, 10, and 17; Asai et al., 2003) are not known to have a specific cleavage recognition site. Of particular relevance is the observation that ADAM10 cleaves prion protein in the region of this protein (residues 106–126) known to drive prion multimerization and eventually fibril formation (Checler and Vincent, 2002). The observation that both the Aβ sequence and the prion aggregation domain are cleaved by  $\alpha$ -secretase activity suggests that the parental proteins containing these domains may be subject to similar proteolytic regulation. Thus, these domains, despite their lack of sequence similarity, may have analogous functions. The ADAM10 cleavage site in prion protein (NMKH<sup>V</sup>MAGA) has no sequence identity with the ADAM10 cleavage site in APP (HHQK<sup>V</sup>LVFF), consistent with the hypothesis that  $\alpha$ -secretase substrate recognition may depend on higher-level protein structure (e.g., multimerization or  $\beta$ -sheet formation) rather than on primary sequence. Studies with the related metalloproteinase ADAMTS-4 also highlight the importance of overall protein structure, rather than specific primary sequence, in cleavage site selection by this class of proteases (Lauer-Fields et al., 2007). These observations support the view that the effects of the Leu<sup>613</sup>Pro substitution act through influencing APP quaternary structure rather than changing local epitopes.

An alternative mechanism by which the Leu<sup>613</sup>Pro substitution could alter APP processing would be through modulating the intracellular trafficking of APP. A recent study has shown that the natural "Arctic" FAD mutation of APP (Glu<sup>618</sup>Gly in APP695, Glu<sup>22</sup>Gly in Aβ) alters the trafficking of APP, resulting in decreased accumulation

of cell surface APP and increased production of intracellular A $\beta$  (Sahlin et al., 2007). However, we have not detected a significant difference in cell surface accumulation between APP695 and APP695 Leu<sup>613</sup>Pro. Although we cannot exclude the possibility that the Leu<sup>613</sup>Pro substitution interferes with the binding of some unknown protein(s) that modulate APP processing, the simplest interpretation of our data is that this substitution acts by altering the conformation of the parent protein.

Extracellular A $\beta$  peptide has been reported to promote the dimerization of membrane bound APP or the APP C-terminal fragment resulting from  $\beta$ -secretase cleavage, with a subsequent decrease in cell viability (Shaked et al., 2006). This interaction occurs between the A $\beta$  peptide and its cognate sequences in the extracellular portion of APP (i.e., APP 597–624). Thus, the aggregation capacity of the A $\beta$  sequence may also play a role in the modulation of APP function by extracellular A $\beta$ .

### Acknowledgments

We would like to thank A. Bergman for providing the C99-GVP and UAS plasmids, and V. Galvan for providing both the APP695 plasmid and extensive experimental advice. The JLA20 monoclonal antibody was obtained from the Developmental Studies Hybridoma Bank developed under the auspices of the NICHD. We would also like to thank J. Yerg III, D. R. Kipp, and E. Wagner for their technical help during the course of this project, and J. Springett for the media preparation. This work was supported by NIH grants AG12423 and AG21037 to C.D.L.

### References

- Asai, M., Hattori, C., Szabo, B., Sasagawa, N., Maruyama, K., et al., 2003. Putative function of ADAM9, ADAM10, and ADAM17 as APP alpha-secretase. *Biochem. Biophys. Res. Commun.* 301, 231–235.
- Banker, G., Goslin, K., 1998. *Culturing Nerve Cells*, 2nd edition. MIT Press.
- Bergman, A., Religa, D., Karlstrom, H., Laudon, H., Winblad, B., et al., 2003. APP intracellular domain formation and unaltered signaling in the presence of familial Alzheimer's disease mutations. *Exp. Cell Res.* 287, 1–9.
- Checler, F., Vincent, B., 2002. Alzheimer's and prion diseases: distinct pathologies, common proteolytic denominators. *Trends Neurosci.* 25, 616–620.
- Cupers, P., Orlans, I., Craessaerts, K., Annaert, W., De Strooper, B., 2001. The amyloid precursor protein (APP)-cytoplasmic fragment generated by gamma-secretase is rapidly degraded but distributes partially in a nuclear fraction of neurones in culture. *J. Neurochem.* 78, 1168–1178.
- DePace, A.H., Santoso, A., Hillner, P., Weissman, J.S., 1998. A critical role for amino-terminal glutamine/asparagine repeats in the formation and propagation of a yeast prion. *Cell* 93, 1241–1252.
- Fay, D.S., Fluet, A., Johnson, C.J., Link, C.D., 1998. *In vivo* aggregation of beta-amyloid peptide variants. *J. Neurochem.* 71, 1616–1625.
- Finder, V.H., Glockshuber, R., 2007. Amyloid-beta aggregation. *Neurodegener. Dis.* 4, 13–27.
- Hardy, J., Selkoe, D.J., 2002. The amyloid hypothesis of Alzheimer's disease: progress and problems on the road to therapeutics. *Science* 297, 353–356.
- Jarrett, J.T., Lansbury Jr., P.T., 1993. Seeding "one-dimensional crystallization" of amyloid: a pathogenic mechanism in Alzheimer's disease and scrapie? *Cell* 73, 1055–1058.
- Kaden, D., Munter, L.M., Joshi, M., Treiber, C., Weise, C., et al., 2008. Homophilic interactions of the amyloid precursor protein (APP) ectodomain are regulated by the loop region and affect beta-secretase cleavage of APP. *J. Biol. Chem.* 283, 7271–7279.
- Kamenetz, F., Tomita, T., Hsieh, H., Seabrook, G., Borchelt, D., et al., 2003. APP processing and synaptic function. *Neuron* 37, 925–937.
- Kametani, F., 2004. Secretion of long Abeta-related peptides processed at epsilon-cleavage site is dependent on the alpha-secretase pre-cutting. *FEBS Lett.* 570, 73–76.
- Karlstrom, H., Bergman, A., Lendahl, U., Naslund, J., Lundkvist, J., 2002. A sensitive and quantitative assay for measuring cleavage of presenilin substrates. *J. Biol. Chem.* 277, 6763–6766.
- Kimberly, W.T., Zheng, J.B., Guenette, S.Y., Selkoe, D.J., 2001. The intracellular domain of the beta-amyloid precursor protein is stabilized by Fe65 and translocates to the nucleus in a notch-like manner. *J. Biol. Chem.* 276, 40288–40292.
- Koo, E.H., Lansbury Jr., P.T., Kelly, J.W., 1999. Amyloid diseases: abnormal protein aggregation in neurodegeneration. *Proc. Natl. Acad. Sci. U. S. A.* 96, 9989–9990.
- Kume, H., Maruyama, K., Kametani, F., 2004. Intracellular domain generation of amyloid precursor protein by epsilon-cleavage depends on C-terminal fragment by alpha-secretase cleavage. *Int. J. Mol. Med.* 13, 121–125.
- Lauer-Fields, J.L., Minond, D., Sritharan, T., Kashiwagi, M., Nagase, H., Fields, G.B., 2007. Substrate conformation modulates aggrecanase (ADAMTS-4) affinity and sequence specificity. Suggestion of a common topological specificity for functionally diverse proteases. *J. Biol. Chem.* 282, 142–150.
- Leissring, M.A., Murphy, M.P., Mead, T.R., Akbari, Y., Sugarman, M.C., et al., 2002. A physiologic signaling role for the gamma-secretase-derived intracellular fragment of APP. *Proc. Natl. Acad. Sci. U. S. A.* 99, 4697–4702.
- Li, L., Lindquist, S., 2000. Creating a protein-based element of inheritance. *Science* 287, 661–664.
- Link, C.D., 1995. Expression of human beta-amyloid peptide in transgenic *Caenorhabditis elegans*. *Proc. Natl. Acad. Sci. U. S. A.* 92, 9368–9372.
- Link, C.D., Johnson, C.J., Fonte, V., Paupard, M., Hall, D.H., et al., 2001. Visualization of fibrillar amyloid deposits in living, transgenic *Caenorhabditis elegans* animals using the sensitive amyloid dye, X-34. *Neurobiol. Aging* 22, 217–226.
- Link, C.D., Fonte, V., Hiester, B., Yerg, J., Ferguson, J., et al., 2006. Conversion of green fluorescent protein into a toxic, aggregation-prone protein by C-terminal addition of a short peptide. *J. Biol. Chem.* 281, 1808–1816.
- Moulder, K.L., Onodera, O., Burke, J.R., Strittmatter, W.J., Johnson Jr, E.M., 1999. Generation of neuronal intranuclear inclusions by polyglutamine-GFP: analysis of inclusion clearance and toxicity as a function of polyglutamine length. *J. Neurosci.* 19, 705–715.
- Munter, L.M., Voigt, P., Harmeyer, A., Kaden, D., Gottschalk, K.E., et al., 2007. GxxxG motifs within the amyloid precursor protein transmembrane sequence are critical for the etiology of Abeta42. *EMBO J.* 26, 1702–1712.
- Osherovich, L.Z., Weissman, J.S., 2001. Multiple Gln/Asn-rich prion domains confer susceptibility to induction of the yeast [PSI(+)] prion. *Cell* 106, 183–194.
- Osherovich, L.Z., Cox, B.S., Tuite, M.F., Weissman, J.S., 2004. Dissection and design of yeast prions. *Plos. Biol.* 2, E86.
- Ren, Z., Schenk, D., Basi, G.S., Shapiro, I.P., 2007. Amyloid beta-protein precursor juxtamembrane domain regulates specificity of gamma-secretase-dependent cleavages. *J. Biol. Chem.* 282, 35350–35360.
- Sahlin, C., Lord, A., Magnusson, K., Englund, H., Almeida, C.G., et al., 2007. The Arctic Alzheimer mutation favors intracellular amyloid-beta production by making amyloid precursor protein less available to alpha-secretase. *J. Neurochem.* 101, 854–862.
- Satyal, S.H., Schmidt, E., Kitagawa, K., Sondheimer, N., Lindquist, S., et al., 2000. Polyglutamine aggregates alter protein folding homeostasis in *Caenorhabditis elegans*. *Proc. Natl. Acad. Sci. U. S. A.* 97, 5750–5755.
- Scheuermann, S., Hamsch, B., Hesse, L., Stumm, J., Schmidt, C., et al., 2001. Homodimerization of amyloid precursor protein and its implication in the amyloidogenic pathway of Alzheimer's disease. *J. Biol. Chem.* 276, 33923–33929.
- Shaked, G.M., Kummer, M.P., Lu, D.C., Galvan, V., Bredesen, D.E., Koo, E.H., 2006. Abeta induces cell death by direct interaction with its cognate extracellular domain on APP (APP 597–624). *FASEB J.* 20, 1254–1256.
- Si, K., Lindquist, S., Kandel, E.R., 2003. A neuronal isoform of the aplysia CPEB has prion-like properties. *Cell* 115, 879–891.
- Ter-Avanesyan, M.D., Kushnirov, V.V., Dagkesamanskaya, A.R., Didichenko, S.A., Chernoff, Y.O., et al., 1993. Deletion analysis of the SUP35 gene of the yeast *Saccharomyces cerevisiae* reveals two non-overlapping functional regions in the encoded protein. *Mol. Microbiol.* 7, 683–692.
- True, H.L., Lindquist, S.L., 2000. A yeast prion provides a mechanism for genetic variation and phenotypic diversity. *Nature* 407, 477–483.
- Wurth, C., Guimard, N.K., Hecht, M.H., 2002. Mutations that reduce aggregation of the Alzheimer's Abeta42 peptide: an unbiased search for the sequence determinants of Abeta amyloidogenesis. *J. Mol. Biol.* 319, 1279–1290.